



# Effect of Cu doping on the magnetic and magnetocaloric properties in the HoNiAl intermetallic compound



L. Cui<sup>a</sup>, L.C. Wang<sup>b</sup>, Q.Y. Dong<sup>a</sup>, F.H. Liu<sup>c</sup>, Z.J. Mo<sup>d</sup>, Y. Zhang<sup>a,b</sup>, E. Niu<sup>b</sup>, Z.Y. Xu<sup>b</sup>, F.X. Hu<sup>b</sup>, J.R. Sun<sup>b</sup>, B.G. Shen<sup>b,\*</sup>

<sup>a</sup> Department of Physics, Capital Normal University, Beijing 100048, China

<sup>b</sup> State Key Laboratory for Magnetism, Institute of Physics, Chinese Academy of Sciences, Beijing 100190, China

<sup>c</sup> National Space Science Center, Beijing 100190, China

<sup>d</sup> School of Material Science and Engineering, Hebei University of Technology, Tianjin 300401, China

## ARTICLE INFO

### Article history:

Received 11 October 2013

Received in revised form 21 August 2014

Accepted 21 August 2014

Available online 13 October 2014

### Keywords:

HoNi<sub>1-x</sub>Cu<sub>x</sub>Al

Magnetic properties

Magnetocaloric effect

## ABSTRACT

The magnetic properties and magnetocaloric effect of Cu doping on HoNiAl (HoNi<sub>1-x</sub>Cu<sub>x</sub>Al) have been investigated. Two transitions occurred for samples with  $x = 0$  and  $x = 0.1$  induced by the combination and competition between antiferromagnetic (AFM) and ferromagnetic (FM) orderings. Simple AFM orderings were found in samples with  $x = 0.2$  to  $x = 0.7$  while FM orderings were found in samples with  $x = 0.8$ – $1$ . The magnetocaloric effect (MCE) was investigated in selected samples with  $x = 0.3$  and  $0.8$ . Large magnetic entropy changes ( $\Delta S_M$ ) as  $-29.2$  J/kg K at 9 K and  $-19.7$  J/kg K at 9 K with corresponding refrigerant capacity (RC) of 299 J/kg, 309 J/kg for a field change of 0–50 kOe were observed. The large  $\Delta S_M$  and RC without hysteresis loss indicated these materials attractive candidates for magnetic refrigeration in low temperature range.

© 2014 Elsevier B.V. All rights reserved.

## 1. Introduction

In recent years, magnetocaloric effect (MCE) has stirred enthusiasm of so many researchers for its merits of high efficiency and eco-friendly over commonly used gas compression technique [1–5]. Gd<sub>5</sub>Si<sub>2</sub>Ge<sub>2</sub> [3], La(Fe, Si)<sub>13</sub> [4] and Mn-based Heusler alloys [5] were extensively studied for their potential application as magnetic refrigeration at room temperature. Except for these materials, numerous materials such as PrGa [6], R<sub>2</sub>CuSi<sub>3</sub> [7], Eu<sub>4</sub>PdMg [8], GdCoAl [9], Ho(Co<sub>1-x</sub>Al<sub>x</sub>)<sub>2</sub> [10], La<sub>0.5</sub>Ca<sub>0.4</sub>Li<sub>0.1</sub>MnO<sub>3</sub> [11], RCu<sub>2</sub>Si<sub>2</sub> and RCu<sub>2</sub>Ge<sub>2</sub> (R = Ho, Er) [12], R<sub>15</sub>Si<sub>9</sub>C [13] as well as amorphous alloys [14] have been reported in mainstream magazines in the last few months. On the other hand, RNiAl (R = rare-earth metal) and RCuAl have been extensively studied for their interesting magnetic properties and their capability serving as potential magnetic refrigerants used in cryogenic temperature region and suitable for special applications in space science and so on [15–20]. RNiAl, RCuAl and RNi<sub>1-x</sub>Cu<sub>x</sub>Al all crystallized in the same hexagonal ZrNiAl-type structure and belonged to a large group of RTX family (R = rare-earth metal, T = transition metal, X = p-metal) [15–22]. For RNiAl and RCuAl compounds, a basal plane layer consisted of all the R

atoms and one-third of T atoms while the other nonmagnetic layer made up by all the X atoms and the rest T atoms. These two layers stacked alternately along the c-axis [15–22]. Nowadays, many research works related to the doping at R site and T site have been reported. The results indicated that complex magnetic properties exist in RNi<sub>1-x</sub>Cu<sub>x</sub>Al in which R = Tb, Dy and Er have been systematically investigated [20–22]. In RNi<sub>1-x</sub>Cu<sub>x</sub>Al compounds with R = Tb, Dy and Er, loss of long range ordering were determined for samples with  $x = 0.6$  and  $x = 0.8$ . In addition, the evolution of magnetism in RNi<sub>1-x</sub>Cu<sub>x</sub>Al from RNiAl to RCuAl was rather complex and these magnetic phenomena have been explained by the RKKY interaction [20–22]. But until now, the magnetic and MCE properties of HoNi<sub>1-x</sub>Cu<sub>x</sub>Al compounds have not been reported to the best of our knowledge. In this paper, we systematically investigated the magnetic properties of HoNi<sub>1-x</sub>Cu<sub>x</sub>Al compounds. In addition, MCE properties of HoNi<sub>1-x</sub>Cu<sub>x</sub>Al with  $x = 0.3$  and  $0.8$  were studied and excellent performances have been found in these materials.

## 2. Experimental

The HoNi<sub>1-x</sub>Cu<sub>x</sub>Al specimens were fabricated by arc melting stoichiometric Ho, Cu, Ni and Al with purity better than 99.9 wt.%, under the protection of high-purity argon atmosphere. 3 wt.% excessive of Ho component was used to equalize the weight loss due to the volatilization of the rare earth element in the arc melting process. For ensuring better homogeneity, the samples were turned upside-down and re-melted for four times. Then the buttons were annealed at 973 K for 30 days

\* Corresponding author. Tel.: +86 010 82648082.

E-mail address: [shenbg@aphy.iph.ac.cn](mailto:shenbg@aphy.iph.ac.cn) (B.G. Shen).

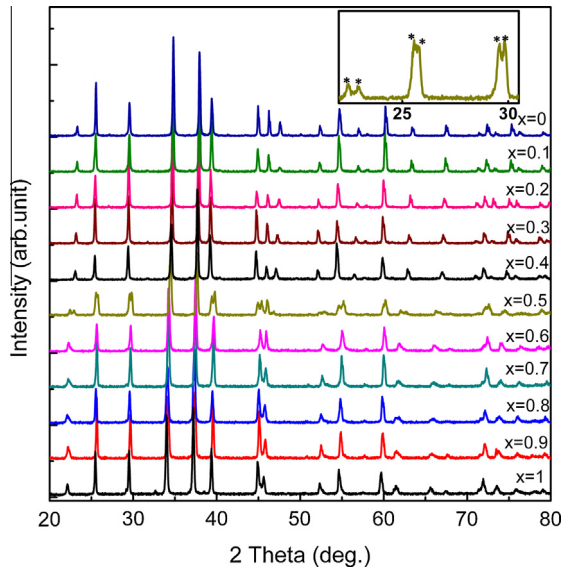


Fig. 1. X-ray diffraction (XRD) patterns for  $\text{HoNi}_{1-x}\text{Cu}_x\text{Al}$  compounds.

in a evacuated quartz tube. Powder X-ray diffraction (XRD) was performed on a commercial D2 diffractometer manufactured by the Bruker Inc. by using  $\text{Cu K}\alpha$  radiation. The magnetic measurements were carried out on the superconducting quantum interference device magnetometer (MPMS, Quantum Design). The isothermal magnetization curves as a function of magnetic field were collected in

heating process. Every time before measuring the next higher temperature, the magnetic field should be oscillated to 0 Oe from 30 kOe to avoid the trapped magnetic field of the instrument.

### 3. Results and discussion

The collected powder XRD patterns for  $\text{HoNi}_{1-x}\text{Cu}_x\text{Al}$  samples as shown in Fig. 1 were examined and the results indicated that all samples were of high quality and crystallized in a hexagonal  $\text{ZrNiAl}$ -type structure (space group  $P62m$ , NO. 189) except for  $x = 0.5$  with impurity phases. The enlarged XRD patterns for  $x = 0.5$  sample was plotted in the inset of Fig. 1. Compared with the other samples, some single peaks in  $x = 0.5$  sample split into two peaks. For obtaining a high quality sample with  $x = 0.5$ , we synthesized series of samples with different excessive amount of Ho and annealed at different temperatures as well as various duration times, but all attempts have failed and the main reason was the split of the single peaks. The concrete reason for this failure needed more experiments and should be declared in the future.

The dependence of magnetization on temperatures ( $M-T$ ) under fixed field was shown in Fig. 2. The solid circles displayed the data collected in the zero-field cooling (ZFC) mode and the hollow circles presented the data recorded in the field-cooling (FC) mode. When compared with other samples, there were two transition temperatures at 5.7 K and 12.8 K in  $x = 0.1$  sample as shown in Fig. 2(a), which was similar to the undoped compound  $\text{HoNiAl}$  [23,24]. Similar result was also reported in  $\text{DyNiAl}$  compound

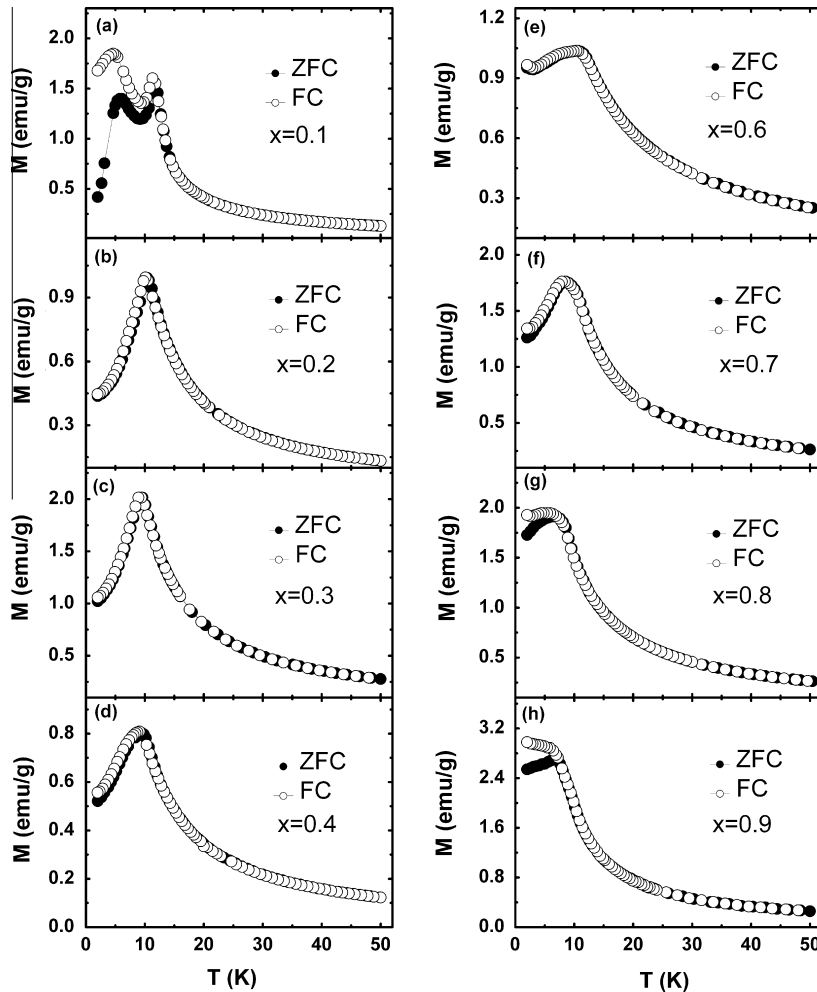


Fig. 2. Temperature dependence of magnetization measured in ZFC and FC modes for  $\text{HoNi}_{1-x}\text{Cu}_x\text{Al}$  compounds under the field of 0.1 kOe.

**Table 1**  
Summary of magnetic properties of HoNi<sub>1-x</sub>Cu<sub>x</sub>Al compounds.

Sample	Type of magnetic ground state	$\theta_p$ (K)	$\mu_{eff}$ ( $\mu_B$ )	$T_{ord}$ (K)	$-\Delta S$ (J/kg K)		RC (J/kg)	
					(0–2 T)	(0–5 T)	(0–2 T)	(0–5 T)
X = 0 [14]	AFM&FM	8.9	10.75	5/13	11.8	24.1	80	310
X = 0.1	AFM&FM	5.9	10.78	5.7/12.8	10.3	23.5	98	330
X = 0.2	AFM	5.8	10.89	10.1	–	–	–	–
X = 0.3	AFM	4.1	11.33	10.5	12.3	28.7	80	285
X = 0.4	AFM	3.6	10.77	9.1	–	–	–	–
X = 0.5	AFM?	–	–	?	–	–	–	–
X = 0.6	AFM	–0.2	11.31	10.7	–	–	–	–
X = 0.7	AFM	3.4	11.17	8.4	–	–	–	–
X = 0.8	FM	2.1	11.36	6.9	9.5	19.6	84	323
X = 0.9	FM	3.6	11.27	9.6	–	–	–	–
X = 1 [20]	FM	10.1	9.6	12	17.5	30.6	178	486

[25]. In our experiment, it was reasonable to assume the similarity between HoNiAl and HoNi<sub>0.9</sub>Cu<sub>0.1</sub>Al for only 10 at.% of Ni was substituted by Cu. Two magnetic phase transitions occurred at 5 K and 14 K that have been detected in the  $M$ – $T$  curves by Suresh et al. [23]. On the other hand, neutron scattering study on HoNiAl indicated the presence of two magnetic phases with transition temperatures around 5 K and 13 K [24]. Within the experimental error, these results concerning the magnetic phase transition agreed well with each other. The earlier neutron scattering study has declared that both ferromagnetic (FM) and anti-ferromagnetic (AFM) components coexisted in the two phases of HoNiAl. To be precise, the FM component was always along the  $c$ -axis while the AFM component lay in the  $a$ – $b$  basal plane for  $T < 5$  K and parallel to  $c$ -axis when  $T > 5$  K [24]. Based on this model, the curve in Fig. 2(a) could be tentatively explained as follows: similar to HoNiAl, the FM component always ordered along the  $c$ -axis while the AFM component lay in the  $a$ – $b$  basal plane for  $T < 5.7$  K and parallel to  $c$ -axis when  $T > 5.7$  K. In the temperature range of  $T < 5.7$  K, the AFM component achieved dominance over FM component and determined the magnetic structure; in the temperature range between the two peaks, the FM and AFM components ordered in the same direction and competed with each other. With the increasing temperature, the FM component took predominant position. For Fig. 2(b)–(h), just one transition temperature that was regarded as AFM ordering was observed for each sample with  $x = 0.2$  to  $x = 0.7$  respectively. For  $x = 0.8$  sample, the magnetization in FC mode below 6.4 K was nearly a constant and just became little smaller with the decreasing temperature and a cocking up behavior emerged below 3 K after a careful examination. The decreasing magnetization might be classified as weak AFM ordering or it stemmed from the complex behavior of Ho<sup>3+</sup> ion in low temperature range, and the conclusion would be determined in the next part. Moreover, the cocking up behavior also existed in samples with  $x = 0.6$  and  $x = 0.7$  in low temperature range. Taking into account of the similar behavior in  $x = 0.8$  sample, this collective behavior could be attributed to the complex behavior of Ho<sup>3+</sup> ion, and more experiments should be made to verify this phenomena. For the sample with  $x = 0.9$ , obvious FM ordering was detected for the magnetization in the FC mode increased with the decreasing temperature. Another phenomenon that caught our sight was that the ZFC curves and FC curves of samples with AFM ordering were nearly overlapped whereas the ZFC curves and FC curves for the samples with FM ordering were irreversible. Reversibility between ZFC curves and FC curves was common for the samples with AFM ordering, while it was generally thought that the thermo-magnetic irreversibility was always observed in a narrow-domain wall pinning system and/or a frustrated system as well as narrow-domain wall pinning compounds [23,25]. Taking into account of the large anisotropy and low transition temperatures of HoNi<sub>1-x</sub>Cu<sub>x</sub>Al samples, the irreversibility could be attrib-

uted to narrow-domain wall pinning effect or the canted magnetic structure of HoNi<sub>1-x</sub>Cu<sub>x</sub>Al. What differed HoNi<sub>1-x</sub>Cu<sub>x</sub>Al from the other RNi<sub>1-x</sub>Cu<sub>x</sub>Al ( $R = \text{Tb, Dy, Er}$ ) compounds was the Cu doping amount boundary for different magnetism. Different boundary was also found in NdNi<sub>1-x</sub>Cu<sub>x</sub>Al system [26]. In view of the current data, the sample with  $x = 0.5$  could be classified as AFM ordering and neutron scattering study should be made to confirm the existence or absence of short range ordering in these compounds that have been found in other RNi<sub>1-x</sub>Cu<sub>x</sub>Al ( $R = \text{Tb, Dy, Er}$ ) compounds. For a comprehensive cognition of these series materials, their magnetic ground state and transition temperatures

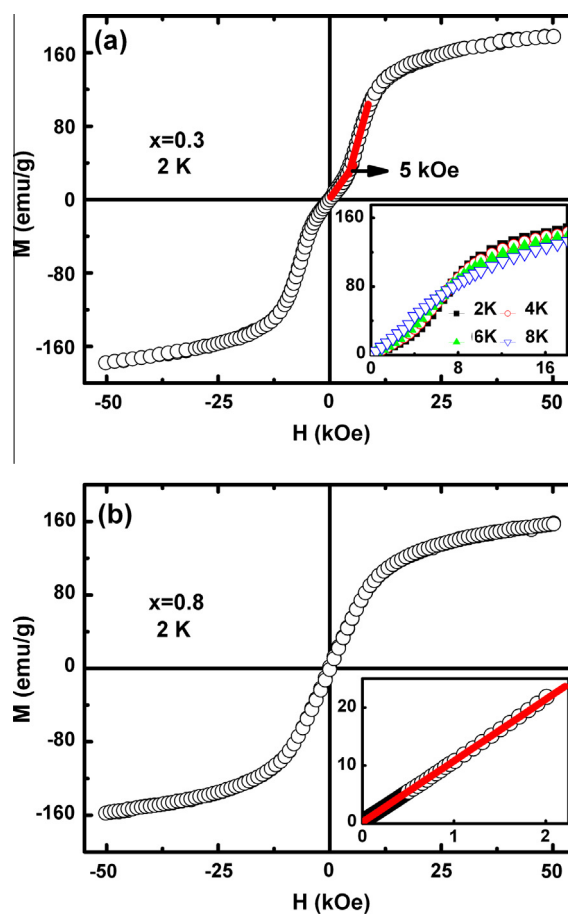


**Fig. 3.** Magnetic hysteresis loops at 2 K up to 50 kOe for (a)  $x = 0.3$  and (b)  $x = 0.8$  respectively with the insets showing the initial magnetization curves at typical temperatures.

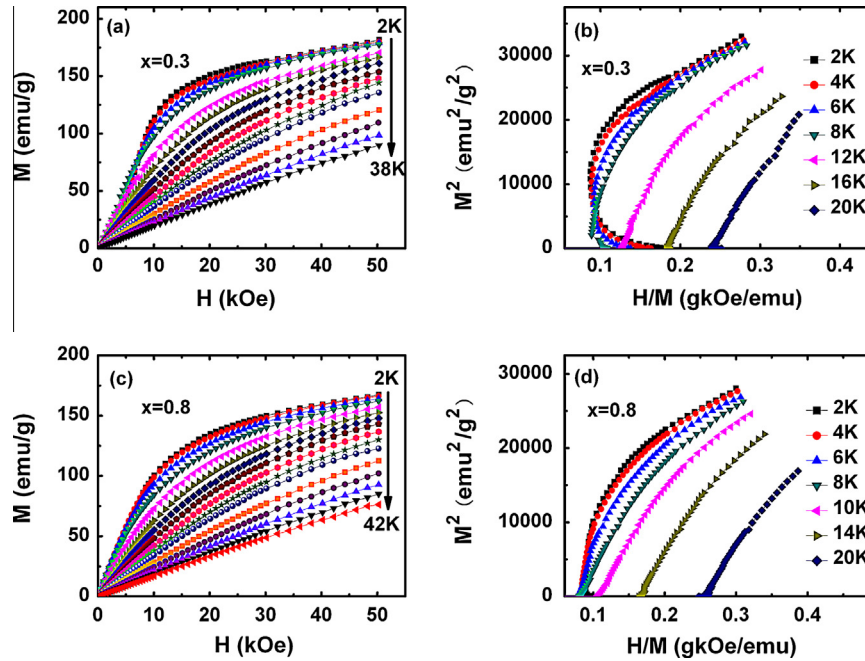


Fig. 4. Magnetic isothermals and Arrott-plots of  $\text{HoNi}_{1-x}\text{Cu}_x\text{Al}$  compounds measured during field increase.

as well as the data derived from the Curie–Weiss fit were listed in Table 1.

Fig. 3(a) and (b) exhibited the magnetic hysteresis loops at 2 K corresponding to samples with  $x = 0.3$  and  $x = 0.8$ , respectively. An obvious change was detected in the slope of the curve at the field of 5 kOe as shown in Fig. 3(a), which was generally thought as a sign of classic metamagnetic transition. The inset of Fig. 3(a) showed the initial magnetization curves ranging from 2 K to 8 K. The crossovers among the curves also verified the AFM ordering in this compound. We have mentioned that the cocking up curve in Fig. 2(g) may come from the weak AFM ordering in the sample or the complex magnetic behavior of  $\text{Ho}^{3+}$  ion in low temperature range. For the purpose to confirm whether AFM ordering exist in  $x = 0.8$  sample, dense data were collected and plotted in the inset of Fig. 3(b). No clue of metamagnetic transition was found and the magnetic ground state for  $x = 0.8$  sample might be classified to FM ordering and the cocking up behavior might be attribute to the complex magnetic behavior of  $\text{Ho}^{3+}$  ion in low temperature range. The saturation magnetic moment determined by extrapolating  $1/H$  to 0 using the  $M-H$  curves measured at 5 K were equal to 10 and  $9.3 \mu_B$  for  $x = 0.3$  and  $x = 0.8$  samples, respectively. These values were so near to the expected  $gJ$  value of  $10 \mu_B$  for free  $\text{Ho}^{3+}$  ion. In addition, negligible hysteresis effect was found in these two samples which was very favorable for the practical application of magnetic refrigerant.

Fig. 4(a)–(d) showed the isothermal magnetization curves as a function of magnetic field and the corresponding Arrott-plots ( $M^2$  VS  $H/M$ ) around their transition temperatures for selected  $\text{HoNi}_{1-x}\text{Cu}_x\text{Al}$  compounds with  $x = 0.3$  and 0.8. Except for the curvature behavior of the isotherms below the transition temperatures that was a feature of ordered state, some isothermal magnetization curves above the transition temperatures also exhibited curvature behavior. Similar results have also been observed in  $\text{HoNiAl}$  and the other intermetallic alloys, which was attributed to the magnetic polaronic-like effect that stemmed from the polarization of 3d band of Ni and have been confirmed by the neutron-diffraction studies [23]. The negative slope of the Arrott plot below  $T_N$  as shown in Fig. 4(b), confirmed the occurrence of a first-order phase transition for  $x = 0.3$  [28]. Generally speaking, metamagnetic transition from AFM ground state to FM state belonged to first

order transition and accounted for the negative slope in Fig. 4(b). The Arrott plots of  $x = 0.8$  as shown in Fig. 4(d) identified the occurrence of a second-order phase transition according to the Banerjee's criterion [28]. On the other hand, as discussed in the previous  $M-T$  results about  $x = 0.8$ , if there exist AFM ordering in sample with  $x = 0.8$ , negative slope related to AFM ordering should be detected in Fig. 4(d). No signs of negative slope detected in Fig. 4(d) confirmed the absence of AFM ordering in sample with  $x = 0.8$  indirectly. The MCE was generally characterized by the iso-

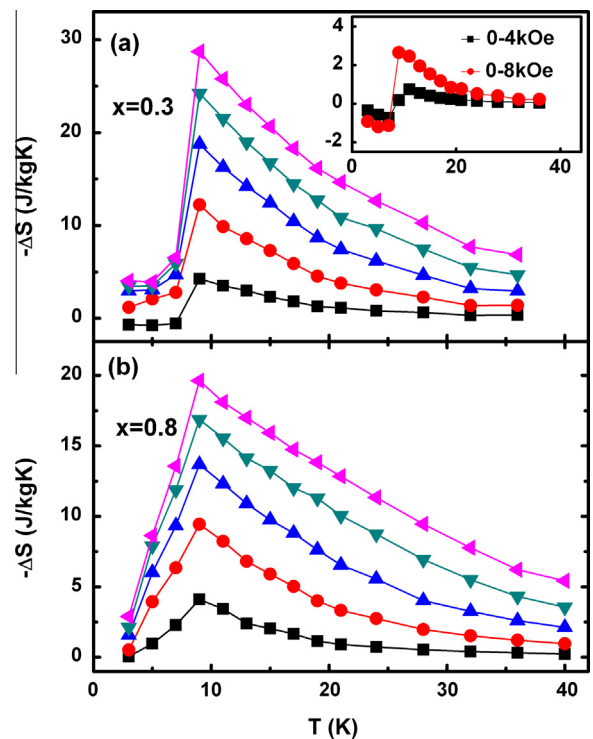


Fig. 5. Magnetic entropy changes as a function of temperature for  $\text{HoNi}_{1-x}\text{Cu}_x\text{Al}$  compounds for various magnetic field changes. The inset of Fig. 4(a) displays the  $\Delta S_M$  under low field changes.

**Table 2**

The ordering temperature, the magnetic entropy change and the refrigerant capacity RC for  $\text{HoNi}_{1-x}\text{Cu}_x\text{Al}$  and some other refrigerant materials.

Sample	Magnetic ground state	$T_{ord}$ (K)	$-\Delta S$ (J/kg K) (0–50 kOe)	RC (J/kg) (0–50 kOe)
$\text{HoNi}_{0.7}\text{Cu}_{0.3}\text{Al}$	AFM	10.5	23.5	330
$\text{HoNi}_{0.2}\text{Cu}_{0.8}\text{Al}$	FM	6.9	19.6	323
$\text{HoCuAl}$ [20]	FM	12	30.6	486
$\text{HoNiAl}$ [14]	AFM&FM	5/13	24.1	310
$\text{ErNi}_{0.8}\text{Cu}_{0.2}\text{Al}$ [21]	AFM	4.6	22.6	257
$\text{ErNi}_{0.5}\text{Cu}_{0.5}\text{Al}$ [21]	FM	5.8	25.9	357
$\text{ErFeSi}$	FM	22	23.1	365
$\text{EuFe}_2\text{As}_2$ [23]	AFM	19	14.6	336
$\text{DyNi}_2$ [24]	FM	21.5	13.5	209
$\text{ErMn}_2\text{Si}_2$ [25]	FM	4.5	25.2	365
$\text{ErRuSi}$ [26]	FM	8	21.2	416
$\text{TmCuAl}$ [27]	FM	4	24.3	373
$\text{HoPdIn}$ [28]	FM	23	14.6	496

thermal magnetic entropy changes ( $\Delta S_M$ ) and the refrigeration capacity (RC). The  $\Delta S$  was always determined by employing Maxwell's relation  $\Delta S = \int_0^H (\partial M / \partial T)_H dH$  while the popular method of calculating the value of RC was to numerically integrate the area under half maximum of  $\Delta S_M$  versus T plot [29–31]. Magnetic entropy changes as a function of temperature for  $\text{HoNi}_{1-x}\text{Cu}_x\text{Al}$  compounds under various magnetic field changes were displayed in Fig. 5. The  $\Delta S_M$  under low magnetic field changes for  $x = 0.3$  sample were plotted in the inset of Fig. 5(a). Positive values of  $\Delta S_M$  were found in the inset of Fig. 5(a), corresponding to the AFM nature of this sample. Unlike the  $x = 0.3$  sample, only negative values were observed in sample with  $x = 0.8$ . The maximum values of  $\Delta S_M$  related to samples with  $x = 0.3$  and  $0.8$  were  $-29.2$  and  $-19.7$  J/kg K with corresponding RC as 299 J/kg, 309 J/kg, for a field change of 0–50 kOe. For comparison, the magnetocaloric properties of  $\text{HoNi}_{1-x}\text{Cu}_x\text{Al}$  and some other refrigerant materials were listed in Table 2. It was evident that the peak values of  $\Delta S_M$  were competitive to the other potential magnetic refrigerant materials in low temperature span under the same field changes [29–37]. For practical application, particular attention should be paid that large  $\Delta S$  values as  $-12.3$  and  $-9.4$  J/kg K with corresponding RC of 80 J/kg and 79 J/kg could be achieved for a low field change of 0–20 kOe, which could be supplied by  $\text{Pr}_2\text{Fe}_{14}\text{B}$  permanent magnet.

#### 4. Conclusions

To summarize, magnetic ground state and transition temperatures of  $\text{HoNi}_{1-x}\text{Cu}_x\text{Al}$  compounds have been determined. Two transition temperatures originated from the coexistence of AFM and FM ordering were found in  $x = 0$  and  $x = 0.1$  samples. AFM ordering were found in samples with  $x = 0.2$  to  $x = 0.7$  while FM ordering were detected in samples with  $x = 0.8$  to  $x = 1$ . The MCE properties were investigated in selected samples and the excellent MCE performance of these compounds were comparable to the other popular potential refrigerants.

#### Acknowledgements

This work was supported by the National Natural Science Foundation of China (11274357, 51021061, 51271196), the Key Research Program of the Chinese Academy of Sciences, the Hi-Tech

Research and Development program of China (2011AA03A404), and the National Basic Research Program of China (2010CB833102), and is a part of the Beijing Excellent talent training support (Grant No. 2012D005016000002).

#### References

- [1] V. Franco, J.S. Blázquez, A. Conde, Appl. Phys. Lett. 89 (2006) 222512–1–3.
- [2] O. Tegus, E. Bruck, K.H.J. Buschow, F.R. de Boer, Nature (London) 415 (2002) 150–152.
- [3] V.K. Pecharsky, K.A. Gschneidner Jr., Phys. Rev. Lett. 78 (1997) 4494–4497.
- [4] B.G. Shen, F.X. Hu, Q.Y. Dong, J.R. Sun, Chin. Phys. B 22 (2013) 017502–1–11.
- [5] F.X. Hu, B.G. Shen, J.R. Sun, Chin. Phys. B 22 (2013) 037505–1–15.
- [6] X.Q. Zheng, J. Chen, Z.Y. Xu, Z.J. Mo, F.X. Hu, J.R. Sun, B.G. Shen, J. Appl. Phys. 115 (2014), 17A938–1–3.
- [7] F. Wang, F.Y. Yuan, J.Z. Wang, T.F. Feng, G.Q. Hu, J. Alloys Comp. 592 (2014) 63–66.
- [8] L.W. Li, Oliver Niehaus, Marcel Kersting, Rainer Pöttgen, Appl. Phys. Lett. 104 (2014), 092416–1–4.
- [9] H. Fu, Z. Ma, X.J. Zhang, D.H. Wang, B.H. Teng, E. Agurto Balfour, Appl. Phys. Lett. 104 (2014), 072401–1–4.
- [10] T.I. Ivanova, S.A. Nikitin, G.A. Tskhadadze, Yu.S. Koshkid'ko, W. Suski, W. Iwasieczko, D. Badurski, J. Alloys Comp. 592 (2014) 271–276.
- [11] R.W. Li, W. Tong, L. Pi, Y.H. Zhang, J. Magn. Magn. Mater. 355 (2014) 276–281.
- [12] Z.J. Mo, J. Shen, L.Q. Yan, X.Q. Gao, L.C. Wang, C.C. Tang, J.F. Wu, J.R. Sun, B.G. Shen, J. Appl. Phys. 115 (2014), 073905–1–6.
- [13] Amitava Bhattacharyya, A. Thamizhavel, S.K. Dhar, P. Manfrinetti, J. Alloys Comp. 588 (2014) 720–724.
- [14] B. Podmiljsak, J.-H. Kim, P.J. McGuinness, S. Kobe, J. Alloys Comp. 591 (2014) 29–33.
- [15] Niraj K. Singh, K.G. Suresh, R. Nirmala, A.K. Nigam, S.K. Malik, J. Magn. Magn. Mater. 302 (2006) 302–305.
- [16] Y.Y. Zhu, Kai Asamoto, Yuta Nishimura, Takaaki Kouen, Satoshi Abe, Koichi Matsumoto, Takenori Numazawa, Cryogenics 51 (2011) 494–498.
- [17] Niraj K. Singh, K.G. Suresh, R. Nirmala, A.K. Nigam, S.K. Malik, J. Appl. Phys. 99 (2006), 08K904–1–3.
- [18] H. Takeya, V.K. Pecharsky, K.A. Gschneidner Jr., J.O. Moorman, Appl. Phys. Lett. 64 (1994) 2739–2741.
- [19] P. Javorský, H. Nakotte, R.A. Robinson, T.M. Kelley, J. Magn. Magn. Mater. 186 (2012) 373–376.
- [20] J. Prchal, P. Javorský, V. Sechovský, M. Dopita, O. Isnard, K. Jurek, J. Magn. Magn. Mater. 283 (2004) 34–45.
- [21] Jiří Prchal, Pavel Javorský, Blanka Detlefs, Stanislav Daniš, Olivier Isnard, J. Magn. Magn. Mater. 310 (2007) e589–e591.
- [22] Jiří Prchal, Takashi Naka, Martin Mišek, Olivier Isnard, Pavel Javorský, J. Magn. Magn. Mater. 316 (2007) e499–e502.
- [23] N.K. Singh, K.G. Suresh, R. Nirmala, A.K. Nigam, S.K. Malik, J. Appl. Phys. 101 (2007), 093904–1–5.
- [24] P. Javorský, P. Burlet, E. Ressouche, V. Sechovský, G. Lapertot, J. Magn. Magn. Mater. 159 (1996) 324–330.
- [25] P. Javorský, L. Havela, V. Sechovský, H. Michor, K. Jurek, J. Alloys Comp. 264 (1998) 38–42.
- [26] Jiří Prchal, Eva Šantavá, David Schmoranz, Physica B 404 (2009) 3056–3058.
- [27] A.V. Andreev, P. Javorský, A. Lindbaum, J. Alloys Comp. 290 (1999) 10–16.
- [28] S.K. Banerjee, Phys. Lett. 12 (1964) 16–17.
- [29] L.C. Wang, Q.Y. Dong, Z.J. Mo, Z.Y. Xu, F.X. Hu, J.R. Sun, B.G. Shen, J. Appl. Phys. 114 (2013), 163915–1–4.
- [30] L.C. Wang, Q.Y. Dong, J. Lu, X.P. Shao, Z.J. Mo, Z.Y. Xu, J.R. Sun, F.X. Hu, B.G. Shen, J. Appl. Phys. 114 (2013), 213907–1–6.
- [31] H. Zhang, B.G. Shen, Z.Y. Xu, J. Shen, F.X. Hu, J.R. Sun, Y. Long, Appl. Phys. Lett. 102 (2013), 092401–1–4.
- [32] M.S. Kim, N.H. Sung, Y. Son, M.S. Ko, B.K. Cho, Appl. Phys. Lett. 98 (2011), 172509–1–3.
- [33] P.J. Ibarra-Gaytan, C.F. Sánchez-Valdes, J.L. Sanchez Llamazares, Pablo Álvarez-Alonso, Pedro Gorria, J.A. Blanco, Appl. Phys. Lett. 103 (2013), 152401–1–5.
- [34] L. Li, K. Nishimura, W.D. Hutchison, Z. Qian, D. Huo, T. Namiki, Appl. Phys. Lett. 100 (2012), 152403–1–4.
- [35] S.B. Gupta, K.G. Suresh, Appl. Phys. Lett. 102 (2013), 022408–1–4.
- [36] Z.J. Mo, J. Shen, L.Q. Yan, J.F. Wu, L.C. Wang, C.C. Tang, B.G. Shen, Appl. Phys. Lett. 102 (2013), 192407–1–4.
- [37] Lingwei Li, Takahiro Namiki, Dexuan Huo, Zhenghong Qian, Katsuhiko Nishimura, Appl. Phys. Lett. 103 (2013), 222405–1–4.